

Kauer, J.S., White, J. 2002. Representation of odor information in the olfactory system: from biology to an artificial nose. In: Sensors and Sensing in Biology and Engineering. Barth, F.G., Humphrey, J.A.C. Secomb, T.W. (eds) Springer Verlag, Berlin

Representation of Odor Information in the Olfactory System: From Biology to an Artificial
Nose

John S. Kauer, PhD and Joel White, PhD

Dept. of Neuroscience
Tufts University School of Medicine
136 Harrison Av.
Boston, MA 02111
Tel: 617-636-3844
Fax: 617-636-0476
Email: john.kauer@tufts.edu

Running head: a biologically inspired, artificial olfactory system
Corresponding author: John S. Kauer, PhD

I. Abstract

II. Introduction

III. From Biology to an Artificial Nose

- A. Odor Coding Mechanisms in the Biological Olfactory System.
- B. Representation of the Coding Hypothesis in a Computer Simulation.
- C. Design of an Artificial Olfactory System Based on Biological Principles.

IV. Conclusion

V. Acknowledgements

VI. References

I. Abstract

The olfactory systems of animals as diverse as insects and primates are well-known for having extraordinary sensitivity while, at the same time, exhibiting broad discriminative abilities. These properties, often mutually exclusive in other chemical recognition systems, appear to arise from the parallel, distributed nature of the processes that underlie how odors are encoded at each level in the olfactory pathway in the brain. In this paper we describe how we have tried to characterize the physiological aspects of these processes in biological experiments, capture these processes in a computational model, and then to use these observations to design and build a biologically inspired artificial device. The Tufts Medical School Nose has achieved a degree of sensitivity and discriminability that, for certain compounds under defined conditions, approaches that of its biological parent.

II. Introduction

Many molecular recognition systems, such as those involved in neurotransmission and gene regulation, trade response diversity for specificity and sensitivity. The more sensitive a receptor system (for example, pheromone receptors in insects or high affinity receptors in the brain), generally the less able it is to recognize a diversity of molecular species. High sensitivity usually implies high selectivity at the cost of broad-band response. If the structure of a compound (or compounds) to be detected is defined, an effective way to build a detector (or detectors) is to make receptors highly specific for that compound (for example, to recognize pheromones). If, however, one requires that a system can recognize a wide diversity of molecular structure and be flexible enough to discriminate among compounds without prior knowledge of their identity, then reliance on highly specific receptors is not advantageous. To have broad discrimination, even with the use of extensive arrays, multitudes of specific receptors must be produced, one for each compound of interest, with the risk that receptors for compounds outside the range of the target set (or that might have future significance), would not be generated. In the vertebrate olfactory pathway the dichotomous requirements of high sensitivity *and* broad-band response seem to have been met by pressures that have evolved an unusual, but highly effective and flexible, chemical detector system.

In this paper we briefly outline a number of features of the air-breathing, vertebrate olfactory system. We then describe a computational model we have devised to represent some of these properties in mathematical terms, and, finally, we show how we have used these properties

to build a device designed to carry out a real-world, low-concentration odor detection task – finding landmines. The first artificial nose developed by Persaud and Dodd (1982) was also inspired by two basic attributes of olfactory function: cross-reactive sensors and pattern recognition. We have extended this approach such that in we have incorporated more than 20 characteristics of olfactory function into our device. The underlying theme of this work is that the requirements for a flexible, highly sensitive, broad-band olfactory system have been satisfied by complementary interactions between primary odorant transduction processes involving relatively non-specific (with regard to overall molecular structure) receptors linked to biochemical cascades and the brain circuits that extract the information necessary for odor-guided behavior of the organism. Some of these ideas that relate to biological olfactory function have also been discussed in other reviews (see Buck, 1996; Hildebrand and Shepherd, 1997; Kauer, 1980; Kauer, 1987; Kauer, 1991; Kauer and Cinelli, 1993; Kauer and White, 2001; Mori et al. 1999; Shepherd, 1994).

III. From Biology to an Artificial Nose

A. Odor Coding Mechanisms in the Biological Olfactory System

The prevailing hypothesis about how odorant molecules are encoded by the nervous system (see reviews above), is that chemical structure is represented by a combinatorial process involving distributed recognition of multiple molecular subcomponents, not by a binding to the global molecular structure of the odorant. The subcomponents of even monomolecular odors (variously called ‘odotopes’ (Shepherd, 1987), in analogy with epitopes in the immune system; ‘olfactophores’ (Ham and Jurs, 1985); or ‘recognition elements’) bind to arrays of olfactory receptors, converting chemical information into electrical neuronal activity. This encoded

information is sequentially propagated to olfactory circuits first in the olfactory bulb and then to higher order olfactory areas in a form that generates spatially and temporally distributed activity patterns at each level of the pathway. This encoding process does not imply that the activity is diffuse, non-specific, chaotic, nor lacking in component structure, rather that, even for monomolecular stimulus compounds, many cells at each level in the brain pathway participates in these odor encoding, re-encoding, and integration processes.

Distribution of activity in this way is reminiscent of 'neural networks' (as this term is used in computer theory; see Kauer, 1991) and provides for many of the well-documented aspects of olfactory function that include high sensitivity accompanied by broad-band response, adaptability to new environments, and fault tolerance upon exposure to injury. This encoding scheme is substantively different from the way chemical recognition is thought to occur in the specific interactions between individual ligands and their high affinity, cognate receptors. We have termed this process 'distributed specificity', in which the fidelity of recognition for a particular odor at the perceptual level emerges from complex events widely distributed in space and time at more peripheral levels. We believe this hypothesis is not only important for studying olfactory function, but also may serve as a paradigm for understanding how other systems in the brain represent information in a distributed fashion.

1. Structure and Function of the Peripheral Olfactory Pathway – This section briefly describes a number of the general features of the peripheral olfactory system as they are seen in the animal model we have worked on, the tiger salamander *Ambystoma tigrinum* (Kauer, 1973). An interesting feature of olfactory systems is the conservation of structure and function across many phyla, such that properties described for the salamander are relevant for a diversity of other species. A large literature on the olfactory system of the tiger salamander (some 160 papers) has

been generated over the last 30 years providing a wealth of data for making direct comparisons among anatomical, physiological, biochemical, molecular biological, and behavioral information from a single species. This animal has numerous experimental advantages including easily obtained physiological signals from a variety of brain regions, robust tissue that tolerates *in vitro* study, large, experimentally accessible neurons, nasal cavity structure that permits controlled odorant stimulation, easily measured odor-guided behavior, relatively well-defined primary receptor and neurotransmitter systems, and molecular receptors similar to those found in the mammal.

- Figure 1 near here -

2. The olfactory epithelium – Fig. 1 shows a simplified diagram of the first stages in the olfactory pathway, the olfactory epithelium (OE) and olfactory bulb (OB). Although in the salamander the nasal chamber is a flattened sac that contrasts with the convoluted and aerodynamically complex nasal cavity of the mammal, the anatomy and physiology of the olfactory sensory neurons (OSNs) and the distribution of odorant receptors (ORs) are remarkably similar. OSNs send dendrites to the epithelial surface where they end in sensory cilia embedded in a layer of mucus. The biochemical machinery for primary odorant transduction, including the ORs and second messenger cascades, is in the cilia. The initial recognition event occurs via binding of an odorant to members of a large family of 7 transmembrane, G-protein linked receptors, that ultimately open cyclic nucleotide gated channels via an adenylate cyclase mediated cascade (see reviews (Ache, 1994; Anholt, 1993; Buck, 1996; Mombaerts, 1999; Schild and Restrepo, 1998)).

In the fish, amphibians, and mammals studied thus far, OSNs expressing one OR phenotype are found scattered within broad, but defined, OE regions or zones (Ressler et al.

1993; Vassar et al. 1994), not in contiguous clusters. Distribution of odorant responses across the OE has been observed using several different recording methods and have consistently shown that, as for the distribution of the ORs, they are broadly, but non-homogeneously distributed across the OE. Precisely how the scattered distributions of ORs relate to the broadly distributed odorant response patterns is still not clearly defined.

In general, OSNs distributed in zones, sequentially depolarize as the bolus of odor moves through the nasal cavity during a sniff. This generates barrages of temporally patterned action potentials in multitudes of OSN axons that project to the first synapse in the glomeruli of the OB (see boxes A-E, Fig. 1). After binding to ORs in the cilia, the chemical information in the odorant stimulus is now represented in these distributed firing patterns. The general finding is that individual OSNs respond to multiple odorants and that OSNs expressing different ORs can respond to the same odorant. This is the fundamental observation that underlies the combinatorial complexity of the first stage encoding process.

It has been shown that OSNs turn over in all vertebrates studied (Graziadei, 1973) including the salamander (Simmons and Getchell, 1981), yet it is thought that olfactory function generally remains more or less stable throughout life. Any hypothesis of how odorants are encoded by the nervous system must accommodate this turnover process that continues for the lifetime of the organism.

3. Connections to the olfactory bulb – Unlike the regular topographic mapping long recognized as a canonical attribute of other sensory modalities, there has been a question of how the projections of OSN axons in the OE map onto their glomerular targets in the OB. Recent molecular marking experiments (Mombaerts, 1999) have confirmed and extended earlier anatomical and physiological data (Cinelli et al. 1995; Cinelli and Kauer, 1995; Kauer, 1980;

Kauer, 1987; Kauer and Moulton, 1974) and show that the spatially distributed populations of OSNs expressing one OR converge onto one or two glomeruli. These convergence patterns are an essential element for understanding how odorants are encoded and we have included them in our models and engineered devices.

4. The olfactory bulb - Much is known about the structure of the OB circuit, the distribution of neurotransmitters, and odorant and electrical response properties of single OB cells in a number of different animals (for reviews see Christensen and White, 2000; Hildebrand and Shepherd, 1997), including the salamander. These studies show that the OB circuit and responses of the output mitral/tufted (M/T) cells are, as for OSN properties, remarkably conserved through phylogeny. Upon stimulation with an odorant, subsets of M/T cells across the extent of the OB are activated with a limited number of temporal response patterns which relate to odorant concentration and recording site (see examples of intracellular records in Fig. 2 IIAb, Bb, Cb; IIIAb, Bb). Each of these temporal response patterns is seen with all odors tested and thus firing pattern *per se* does not encode odor quality. Like OSNs, each M/T cell generally responds to a number of different compounds in ways that suggest they are encoding some molecular attribute of the odorant. For example, recently it has been observed that rabbit M/T cells (and certain OB locations observed using imaging methods) respond with higher firing rates to molecules (especially fatty acids) having a particular carbon chain length (Friedrich and Korsching, 1998; Mori et al. 1999; Rubin and Katz, 1999; Slotnick et al. 1997; Uchida et al. 2000). These kinds of data support the hypothesis that the characteristic to which these cells respond is likely to be a molecular subcomponent of the compound (i.e. carbon chain length), not the entire molecule.

Overall distributions of OB responses have been observed using electroencephalographic, 2-deoxyglucose (2DG), c-fos, and voltage-sensitive dye (VSD) recording (see reviews Christensen and White, 2000; Hildebrand and Shepherd, 1997; Kauer and White, 2001). Results from these studies consistently show that activity appears in widely distributed loci within and across the layers of the bulb after stimulation with odor. Patterns of activity to defined odorants are relatively consistent across individuals of the same species and generally become more widely distributed with the application of high concentrations.

5. Higher olfactory centers: the piriform cortex, anterior olfactory nucleus, amygdala, olfactory neocortex – There is still relatively little known about how odor information is processed in olfactory areas beyond the OB. Although many details about piriform cortex circuits have been elucidated (Haberly, 2001; Zou et al. 2001), there are few data on odor responses at either single cell or ensemble levels in this structure. Recent experiments in the mammal have shown that adaptation to odorants in the OB and piriform cortex is complex and depends on the frequency of odor delivery and on the state of feedback circuits from one level to another (see Wilson, 1998; Wilson, 2000; Young and Wilson, 1999). These experiments emphasize how sniffing (odorant access) is likely to be an important variable in the coding process. We have included control over stimulus access using brief, defined ‘sniffs’ in our artificial device.

6. Odor-guided behavior - There have been many studies on odor-related behavior in rodents, salamanders, and other animals. Among the most significant for understanding how the system encodes molecular odor information have been those in which odor detection or recognition has been tested after pathway lesion (Hudson, 1999; Hudson and Distel, 1987; Slotnick et al. 1997). In general, these studies show that animals do well on odor detection tasks

even with up to 85% of their OB's removed, indicating a remarkable redundancy in OB circuits in which widely distributed information underlies a robust fault tolerance. We have attempted to capture this property of fault tolerance and redundancy in our computational model and artificial device.

7. An odorant coding hypothesis: A schematic diagram of a number of the attributes of olfactory function and how they relate to our odor coding hypothesis is shown in Fig. 1.

The essential elements of this hypothesis are as follows:

- Individual OSNs respond to several different odorant compounds. This is because they express ORs (a,b,c... in Fig. 1) not responsive to the overall shape, but rather to a substructure (i.e. a recognition element) of the odorant. Recognition of a number of such subcomponents, taken together, are necessary to characterize even single, monomolecular compounds.

- OSNs express one, or a small number of, ORs such that one OSN population expressing one OR phenotype responds to one recognition element; other OSN populations expressing other ORs respond to other recognition elements. A number of different OSN populations thus respond to any one odorant and, conversely, one OSN population responds to as many different odorants as share the recognition element to which its ORs are sensitive, even compounds which may perceptually smell different. The definitive number of ORs expressed and functional at any one time to encode one odorant species is unknown.

- The cells comprising an OSN population expressing one OR are distributed within broad, but defined regions of the OE ('zones'; see encircled regions in the OE in Fig. 1), mixed in among other OSN populations expressing other ORs. Sensory cells expressing one OR are not found as clusters of contiguous cells in uniform patches of epithelium, but are intermixed within a zone (see overlap of encircled regions in the OE in Fig. 1). The relationships of each OSN

population expressing one OR to the temporally and spatially distributed responses elicited by a particular odorant are not well understood.

- Since any one odorant interacts with multiple OSN populations, how much these populations overlap spatially, determines the patterns of distributed activity in the OE that have been observed using 2DG, electroolfactogram, and VSD recording.

- The OE does not map onto the OB in the point-to-point fashion that other senses map onto the central nervous system. Rather, axons from distributed OSNs that express the same OR converge onto one or two glomeruli. See lines coming from a's, b's, and c's converging onto glomeruli (glom) in Fig. 1.

- Groups of M/T cells, with associated interneuronal circuitry, connect with functionally related groups of glomeruli (Fig. 1) and serve as building block modules making up the overall response to an odorant. The ensemble of activated modules (with temporally complex responses, as shown in the descending panels, A – E of Fig. 1 depicting activation of different OB neurons over time) encodes the ensemble of recognition elements expressed by the odorant stimulus in a way similar to how computer 'neural networks' encode distributed information. Distributed activation of the modules is the basis for the widespread patterns of activity observed in 2DG and VSD recordings from the OB. The relationships of these modules to specific OSN populations and to particular molecular features is beginning to be determined.

- A module responding to a recognition element consists of M/T (and other OB) cells that are both excited and inhibited in limited numbers of temporal patterns that depend on their role in the circuit. Concentration is coded by temporal patterning of the responses and by the number of cells responding.

This simplified characterization of OE and OB function describes the initial components of odor encoding as being a kind of parallel, distributed processor. We have tried to capture a number of these elements in the formal, mathematical model described in the next section.

B. Representation of the Coding Hypothesis in a Computer Simulation.

Figure 2 shows a brief overview of the OE/OB circuit that we have represented in a computer simulation (I) and illustrates some of the comparisons of the computed results with actual intracellular recordings (II and III). A more complete description of this model can be found in (White et al. 1992). IA shows the essential components of the circuit including 6000 receptor cells (REC); 24 glomerular (GLM) projection targets of the receptor cell axons; 12 periglomerular (PGL) inhibitory interneurons; 12 mitral/tufted (MIT) cells; and 1200 granule (GRL) inhibitory interneurons. The number of cellular elements represented in the model are in similar ratios to one another as are the neurons in the salamander olfactory system, but the absolute numbers are reduced by about one thousand fold (for example, there are estimated to be about 12,000 mitral/tufted cells in the salamander). The connections and spatial relationships among the different cells is a simplified, but accurate, representation of the connections as they are known in this and other animals. The goal of these experiments was to evaluate the degree to which a simplified representation of the peripheral olfactory circuit could generate computed cellular activity that was commensurate with responses observed in real biological neurons. Such comparisons are shown in Fig. 2 II. and III for computed and electrophysiologically measured mitral/tufted cell behavior.

- Figure 2 near here -

Fig. 2 II Aa is an example of a comparison between computed intracellular recordings from two mitral/tufted cells (MIT 6 and MIT 7) and an actual intracellular recording from an identified salamander M/T cell (Fig. II Ab) in response to a single, low intensity, orthodromic electric shock to the afferent olfactory nerve (input to the circuit). One can see that the computed record is remarkably similar to the intracellular record in showing a brief depolarization with an action potential, followed by a period of hyperpolarization. Favorable similarities are also shown for an antidromic electrical stimulation (Fig. 2. IICa,b) and for application of a higher intensity orthodromic shock in Fig. 2. IIBa,b. These records indicate that the simulated circuit captured sufficient detail of the spatially and temporally distributed excitatory and inhibitory interactions that the computed and measured outputs look similar for simple electrical activation of the circuit.

Another test of the ability of the simulation to capture more complex physiological details is shown in Fig. 2 III. Here the computed output represented the results of applying a simulated ‘odor’ to an array of simulated OSNs in spatial patterns depicted by the distributions of the dots on the OE outlines seen in Fig. 2. III Aa and Ba top. Activating the simulated OSNs with these patterns once again generated simulated membrane potential changes in one of the mitral/tufted cells (Fig. 2. III. Aa - MIT 7) that was remarkably similar to that seen in a real intracellular recording after odor stimulation (Fig. 2. III. Ab). In addition to the similarity seen at one concentration, when the simulated odor stimulation was applied at a ‘higher concentration’ the temporal pattern of the computed output changed in a complex way similar to the temporal pattern in the intracellular recording (Fig. 2. IIIBa,b).

Although these simulations are clearly oversimplifications of real biological circuits we were gratified that a number of the essential elements generating spatially and temporally

distributed patterns in M/T cells appeared to have been captured. These simulations made us realize that we could compute spatial/temporal patterns of activity in biologically inspired circuits that would represent both odor quality and concentration. We thus had the basis for a simple ‘artificial olfactory system’. What remained was to add an input stage consisting of sensors that could respond to vapor phase chemicals in the environment, a way to deliver the vapor, and a mechanism to interpret the response patterns.

Among several requirements we had for such sensors was that they be broadly responsive, that is, intentionally non-specific, and that we could generate many different kinds of them. These requirements were met by a class of optically interrogated sensing materials that change their fluorescence when exposed to odorants (Barnard and Walt, 1991; White et al. 1996). These materials consist of intrinsically fluorescent polymers or polymers impregnated with fluorescent dyes that can be made into arrays of discrete sensor sites as described in the next section.

C. Design of an Artificial Olfactory System Based on Biological Principles

The design and development of our artificial olfactory system has been broadly based on the scheme outlined in Fig. 3. After many years of research, we started (Fig. 3, left) with observations on the biological attributes of the olfactory system in a defined experimental model animal, progressed to generating computational simulations of these observations, used computer simulation as a basis for building working hardware prototypes, and finally used (and continue to use) the entire process to focus attention on details of the biological process that might have escaped study had we not been confronted by them in building the engineered device. In this

endeavor, we have extended the approach of Persaud and Dodd (1982), who were the first to build a biologically inspired artificial nose.

- Figure 3 near here –

To identify the components required for building an artificial olfactory system we tried to characterize the essential steps in an olfactory recognition event as shown in Figure 4A. Figure 4B illustrates approximately where each of these steps occurs in biological and artificial systems. We have designed our device to also carry out these steps, albeit more crudely than occurs in the olfactory pathway. Explicit characterization of these events has been an important guide for making the artificial device function effectively and accurate definition of these steps continues to focus future development on critical mechanistic issues.

- Figure 4 near here –

As shown in Fig. 5, the essential elements of the Tufts Medical School Nose consist of an air sampling chamber in which resides an array of optically interrogated vapor phase detectors, a means for delivering vapor phase samples to the sensing array as short ‘sniffs’ (sniff pump), electronic circuits (amplifiers, analogue/digital converters) to detect changes in the optical signals from each sensor (Barnard and Walt, 1991), and a computer to evaluate the matrix of signals from each sensor over time. In this figure vapors from the odor source, gated into discrete pulses by valves (not shown), are drawn from below by a sniff pump (right). The vapor stream passes over the sensing

- Figure 5 near here -

materials (polymers and dyes) which are caused to fluoresce by illumination at the appropriate wavelengths from the array of light emitting diodes (LEDs, at the bottom of the sensing chamber). Changes in fluorescence over the time course of the sniff as a result of the vapor

interacting with the sensing sites are detected by the array of photodiodes (PDs, at the top of the sensing chamber). There is one LED and one PD for each sensing site. This configuration is essentially an array of micro-spectrofluorimeters, each of which is tuned to the wavelengths appropriate for its sensing material. The output of this sensor/detector array consists of a 2 dimensional matrix of numbers in which each column is the signal from one sensor over time. Figure 6 shows such response matrices plotted as topographical surfaces for six different vapor exposure situations. The magnitude of fluorescence change in either the increasing or decreasing direction is plotted on the y-axis. The number of the sensor is plotted on the x-axis (in this case there were 32 sensors) and the time over which data were taken (about 1 sec) is plotted on the z-axis (going into the page). Note that that responses are obtained with short sniffs (about 0.5 sec), that the sensing materials respond rapidly, and that the response surfaces are characteristic and different for each compound tested. The response matrix for each odorant or mixture of odorants is then stored in memory.

- Figure 6 near here -

As used for a real-world odor detection/identification task, the device is ‘trained’ by storing a library of response profiles obtained after sniffing known sources - either pure compounds or complex mixtures such as beer, coffee, or a landmine. When using the device for detecting and identifying unknown odors, sniffs of the unknown source are taken and the response profile is compared to those stored in memory. The matrix in memory to which the profile of the unknown matches best sets the criterion for identification. Statistical methods can be applied to assess the accuracy of the match and a probability that exact identification has been achieved. This is important for knowing the level of certainty when identifying dangerous targets such as landmines having low concentration, ephemeral odor signatures. We have used a number of

algorithms for this matching process and we use a variation of the OE/OB model described above in order to separate concentration from quality information.

We have applied the general approach described above to the problem of finding buried landmines by their odor signature (George et al. 1999). In this task we included fluorescent sensing materials specifically designed by Tim Swager of MIT (Yang and Swager, 1998) for detecting nitroaromatic compounds such as TNT (trinitrotoluene) and DNT (dinitrotoluene), along with other, more broadly responding, materials that allow us to discriminate genuine DNT/TNT from other compounds such as methanol that also give responses in the nitroaromatic sensors.

Under highly controlled and calibrated laboratory conditions at Auburn University (Hartell et al. 1998), we have tested how well our device can detect controlled sources of DNT, TNT and landmine vapors, and discriminate them from background air or methanol. In the tests performed under these conditions the device can detect and discriminate DNT at about 300 parts per trillion. This is below the threshold of most dogs (about 1 part per billion) that have been tested in the same apparatus.

In preliminary trials at a test facility set up by the Defense Advanced Research Projects Agency at Fort Leonard Wood, MO, we have been able to identify the presence of buried landmines (without fuses) when conditions are optimal. Optimal conditions include appropriately warm temperatures, relatively high humidity, and no ambient air movement (wind). Although the device is not yet ready for detecting live mines in real mine fields such as in Afghanistan, these gratifyingly encouraging field results have focused our attention on how to improve the sensitivity and noise immunity of the device. We continue to be guided in this effort by studying and implementing detailed mechanisms of olfactory function revealed in our biological studies.

IV. Conclusion

We have developed an artificial olfactory system based on design principles that have been observed in investigations into the biological sense of smell. At the present time we have incorporated more than 20 such principles into our device (see Table I). These have allowed us to build an apparatus with sufficient sensitivity and discriminability to permit, under certain defined conditions, the detection and identification of nitro-aromatic and other compounds associated with landmines in both laboratory and field settings. Our experience shows that the use of anatomical and physiological observations to guide formulation of mathematical models and the incorporation of these formalized biological principles into a hardware device, can be powerful biomimetic approaches for developing engineered solutions to real-world problems. These studies further indicate that the engineering process required to develop hardware can be an important heuristic process for reciprocally informing the investigation of biological machines (Fig. 3).

V. Acknowledgements: We gratefully acknowledge support for this work from the National Institutes of Health (NIDCD), the Office of Naval Research, and the Defense Advanced Research Projects Agency.

VI. References

Ache B (1994) Towards a common strategy for transducing olfactory information. Seminars in Cell Biology 5: 55-63

- Anholt RR (1993) Molecular neurobiology of olfaction. *Critical Reviews In Neurobiology* 7: 1-22
- Barnard SM and Walt DR (1991) A fibre-optic chemical sensor with discrete sensing sites. *Nature* 353: 338-340
- Buck LB (1996) Information coding in the mammalian olfactory system. *Cold Spring Harbor Symposia on Quantitative Biology* 61: 147-155
- Christensen TA and White J (2000) Representation of olfactory information in the brain In: Finger, TE, Silver WL, and Restrepo D (eds) *The Neurobiology of Taste and Smell*. 197-228
- Cinelli AR, Hamilton KA, and Kauer JS (1995) Salamander olfactory bulb neuronal activity observed by video-rate voltage-sensitive dye imaging. III. Spatio-temporal properties of responses evoked by odorant stimulation. *J.Neurophysiol.* 73: 2053-2071
- Cinelli AR and Kauer JS (1995) Salamander olfactory bulb neuronal activity observed by video-rate voltage-sensitive dye imaging. II. Spatio-temporal properties of responses evoked by electrical stimulation. *J.Neurophysiol.* 73: 2033-2052
- Friedrich RW and Korsching SI (1998) Chemotopic, combinatorial, and noncombinatorial odorant representations in the olfactory bulb revealed using a voltage-sensitive transducer. *Journal of Neuroscience* 18: 9977-9988

- George V, Jenkins T, Leggett D, Cragin J, Phelan J, Oxley J, and Pennington J (1999) Progress on determining the vapor signature of a buried landmine. Proc.13th Ann.Int.Symp.Aerospace/Defense Sensing, Sim.Controls 258-269
- Graziadei PPC (1973) Cell dynamics in the olfactory mucosa. Tissue & Cell 5: 113-131
- Haberly LB (2001) Parallel-distributed processing in olfactory cortex: new insights from morphological and physiological analysis of neuronal circuitry. Chemical Senses 26: 551-576
- Ham CL and Jurs PC (1985) Structure-activity studies of musk odorants using pattern recognition: monocyclic nitrobenzenes. Chem.Senses 10: 491-506
- Hartell M, Myers L, Waggoner L, Hallowell S, and Petrousky J (1998) Design and testing of a quantitative vapor delivery system. Proc.5th Int.Symp.on Anal.Det.Explosives
- Hildebrand JG and Shepherd GM (1997) Mechanisms of Olfactory discrimination: converging evidence for common principles across phyla. Annual Reviews of Neuroscience 20: 595-631
- Hudson R (1999) From molecule to mind: the role of experience in shaping olfactory function. [Review] [80 refs]. Journal of Comparative Physiology A-Sensory Neural & Behavioral Physiology 185: 297-304
- Hudson R and Distel H (1987) Regional autonomy in the peripheral processing of odor signals in newborn rabbits. Brain Res. 421: 85-94

- Kauer JS (1973) Response Properties of single olfactory bulb neurons using odor stimulation of small nasal areas in the salamander. University of Pennsylvania 1-142
- Kauer JS (1980) Some spatial characteristics of central information processing in the vertebrate olfactory pathway. In: van der Starre H (ed) Olfaction and Taste VII. 227-236
- Kauer JS (1987) Coding in the Olfactory system In: Finger TE and Silver WL (eds) Neurobiology of Taste and Smell. 205-231
- Kauer JS (1991) Contributions of topography and parallel processing to odor coding in the vertebrate olfactory pathway. TINS 14: 79-85
- Kauer JS and Cinelli AR (1993) Are there structural and functional modules in the vertebrate olfactory bulb? Micr.Res.and Tech. 24: 157-167
- Kauer JS and Moulton DG (1974) Responses of olfactory bulb neurones to odour stimulation of small nasal areas in the salamander. J.Physiol.(Lond.) 243: 717-737
- Kauer JS and White J (2001) Imaging and coding in the olfactory system. Annual Reviews of Neuroscience 24: 963-979
- Mombaerts P (1999) Molecular biology of odorant receptors in vertebrates. Annual Review of Neuroscience 22: 487-509
- Mori K, Nagao H, and Yoshihara (1999) The olfactory bulb: coding and processing of odor molecule information. Science 286: 711-715

- Persaud K and Dodd G (1982) Analysis of discrimination mechanisms in the mammalian olfactory system using a model nose. *Nature* 299: 352-355
- Ressler KJ, Sullivan SL, and Buck LB (1993) A zonal organization of odorant receptor gene expression in the olfactory epithelium. *Cell* 73: 597-609
- Rubin BD and Katz LC (1999) Optical imaging of odorant representations in the mammalian olfactory bulb. *Neuron* 23: 499-511
- Schild D and Restrepo D (1998) Transduction mechanisms in vertebrate olfactory receptor cells. *Physiological Reviews* 78: 429-466
- Shepherd GM (1987) A molecular vocabulary for olfaction. *Ann.N.Y.Acad.Sci.* 510: 98-103
- Shepherd GM (1994) Discrimination of molecular signals by the olfactory receptor neuron. *Neuron* 13: 771-790
- Simmons PA and Getchell TV (1981) Neurogenesis in olfactory epithelium: loss and recovery of transepithelial voltage transients following olfactory nerve section. *Journal of Neurophysiology* 45: 516-528
- Slotnick BM, Bell GA, Panhuber H, and Laing DG (1997) Detection and discrimination of propionic acid after removal of its 2-DG identified major focus in the olfactory bulb: a psychophysical analysis. *Brain Research* 762: 89-96
- Uchida N, Takahashi YK, Tanifuji M, and Mori K (2000) Odor maps in the mammalian olfactory bulb: domain organization and odorant structural features. *Nat.Neurosci.* 3: 1035-1043

- Vassar R, Chao KC, Sitcheran R, Nunez JM, Vosshall LB, and Axel R (1994) Topographic organization of sensory projections to the olfactory bulb. *Cell* 79: 981-991
- White J, Hamilton KA, Neff SR, and Kauer JS (1992) Emergent properties of odor information coding in a representational model of the salamander olfactory bulb. *Journal of Neuroscience* 12: 1772-1780
- White J, Kauer JS, Dickinson TA, and Walt DR (1996) Rapid analyte recognition in a device based on optical sensors and the olfactory system. *Anal.Chem.* 68: 2191-2202
- Wilson DA (1998) Habituation of odor responses in the rat anterior piriform cortex. *Journal of Neurophysiology* 79: 1425-1440
- Wilson DA (2000) Odor specificity of habituation in the rat anterior piriform cortex. *Journal of Neurophysiology* 83: 139-145
- Yang J-S and Swager TM (1998) Fluorescent porous polymer films as TNT chemosensors: electronic and structural effects. *J.Am.Chem.Soc.* 120: 11864-11873
- Young TA and Wilson DA (1999) Frequency-dependent modulation of inhibition in the rat olfactory bulb. *Neuroscience Letters* 276: 65-67
- Zou Z, Horowitz LF, Montmayeur J-P, Snapper S, and Buck LB (2001) Genetic tracing reveals a stereotyped sensory map in the olfactory cortex. *Nature* 414: 173-179

Figure 1

Simplified schematic diagram of spatial and temporal properties of odorant encoding mechanisms in the peripheral olfactory system of the salamander. Within the large box to the upper right shows an outline of the olfactory epithelium (OE) at the left, with olfactory receptor neurons (OSNs) expressing single olfactory molecular receptors (a,b,c...). These are distributed within defined zones (encircled regions in the OE) and relate to subcomponents of a stylized molecule as shown below left. OSNs connect to the olfactory bulb (OB) with olfactory nerve (on) axon projections that converge from distributed OSNs of one type onto single glomeruli (glom). Other bulbar elements shown include mitral/tufted (m/t) output cells and inhibitory interneuron granule (grl) cells. Inhibitory interneuron periglomerular cells are not shown. The mitral/tufted and granule cells associated with a glomerulus that receives input from a group of OSNs defined by the molecular receptor they express, form a response module. Boxes A – E depict a stylized time series of how the system responds to a bolus of odorant vapor progressing

through the nasal cavity from left to right, sequentially interacting various OSN populations that in turn respond with different spatial and temporal patterns response in different OB modules.

Figure 2

Simulated olfactory epithelium and olfactory bulb circuit (I) and computed and measured responses from salamander mitral/tufted cells (II, III). IA shows the cellular elements used to compute the responses to electrical and odor stimulation shown in II and III. The circuit consists of 6000 receptor cells (REC), 24 glomerular elements (GLM), 12 inhibitory periglomerular cells (PGL), 12 mitral/tufted output cells (MIT), and 1200 inhibitory granule cells (GRL). PGL cells are connected to mitral primary dendrites in the glomeruli via reciprocal dendrodendritic synapses and GRL cells are connected to mitral secondary dendrites via reciprocal dendrodendritic synapses. IB shows the convergent/divergent connectivity patterns from defined epithelial zones onto OB glomeruli. IIA illustrates computed (a) and real (b) intracellular recordings after stimulation of the olfactory nerve with a low intensity electrical shock. Note the similar depolarization with single spike, following hyperpolarization sequence in both computed and measured records. IIB and C show similar comparisons for higher intensity olfactory nerve shock and with antidromic activation of the output axons of mitral/tufted cells. IIIA and B show

similar comparisons for ‘odor’ stimulations. The important observation here is that the dramatic and complex change in temporal patterning occurring with increased odor concentration in the real intracellular recording (compare IIIAb with IIIBb), is replicated in the computed output (compare IIIAa – MIT 7 with IIIBa – MIT 7).

Figure 3

Outline of the procedural approach we have used to implement biological principles in an engineered, artificial olfactory system. This process extends from studying biological mechanisms using standard investigation procedures (anatomy, physiology, etc) to capturing these events in computational models, to implementing biological mechanisms in hardware, and importantly, learning from the engineering process to focus investigation back to the biology.

Figure 4

A. Sequence of steps that occurs in a vapor phase chemical recognition process. B. Block diagram of where the steps in A occur in biological and artificial olfactory systems.

Figure 5

Schematic diagram of the Tufts Medical School artificial olfactory system. The sensing chamber consists of an airway into which are drawn (by the sniff pump, left) the vapors (odor source) to be detected and identified. The sensors consist of an array of light emitting diodes (LEDs), excitation filters, the polymer/dye sensing materials, emission filters, and fluorescence detector photodiodes. In the situation shown here there was a 3 x 3 array of detectors. The changes in fluorescence detected by the photodiodes are amplified, digitized and stored in computer memory. All aspects of the process including sniff generation, modulation of the light sources, modulation of the signals, digitization, and storage of the data are under feedback computer control.

Figure 6

Surface plots of response matrices for six different vapor exposure (stimulus) conditions: blank room air, isopropanol, methanol, amyl acetate, xylene, and dinitrobenzene. This detector array had 32 sensors. Data are plotted with sensor number on the x-axis, change in fluorescence on the y-axis, and time of odor exposure (sniff time) on the z-axis going into the page. Dinitrobenzene was included in this test series because it is a compound found associated with the explosive TNT in landmines. This sensor array included some materials specifically designed for detecting nitroaromatic compounds (see text) as well as other sensors with broader response spectra.

Table I

1. Sensors have broad response spectra distributed within the space of the sample chamber.
2. Sensing device exerts control over environmental attributes of the vapor phase stimulus – humidity, temperature, position in the ambient environment (restricted zone to which sniffing is applied).
3. The vapor phase stimulus is delivered to the detectors in a temporally controlled manner (onset, rise time, duration, fall time, individual sniff frequency, sniff bout frequency).
4. Temporal response profiles are used in pattern analysis algorithms. Temporal patterns are governed by frequency and depth of sniffing, by the response characteristics of the detection circuitry, by duration, intensity, wavelength, rise and fall times of light exposure, and by response properties of sensing materials.
5. Feedback control is exerted over the odorant delivery process in real time when using multiple sniffs per test trial; later sniffs are modulated based on information arriving in early sniffs.

6. Control over the adaptation characteristics of the detectors is accomplished by using short pulse stimuli and by brief and controlled exposure of the detectors to the light source (normalized and controlled bleaching).

7. Long term changes in sensors/detectors are monitored to compensate for changes or deterioration.

8. Consideration of which sensing materials to use is based on their shapes and sizes in 'odor space'. Design of detection system and analytical algorithms is based on the nature of the odorants to be detected.

9. Maximize gain and distance from other sensors in 'odor space' by using measurements of detector response that change non-linearly and are orthogonal to one another along 'odor space' dimensions.

10. Control over sensor material sensitivity is accomplished by a) increasing the surface area of the sensor material; b) increasing surface area and properties of the photodetectors; c) improving intrinsic sensitivity of sensor materials.

11. Sensor responses are stabilized by continuous oscillatory application of ambient odors and of target analyte. Continuous sniffing throughout test session.

12. Multiple sensor mechanisms are used for detection (intrinsic fluorescence of designed materials; fluorescence provided by addition of extrinsic dye).

13. Data from sensors are selectively weighted by feedback from analytical algorithms to optimize the information content that each sensor contributes to defining the odor signature.

14. Gain compression.

15. Ambient odorant interference is controlled by subtraction of background (adaptation).

16. Information transfer from the detectors to analytical circuits is clocked by the sniff cycle.

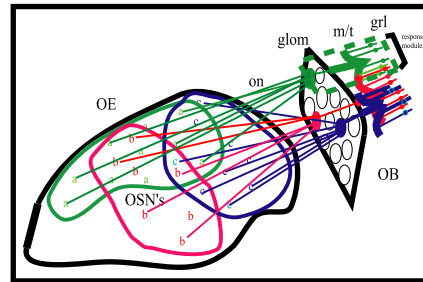
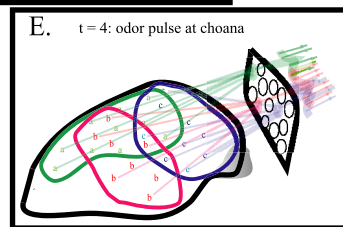
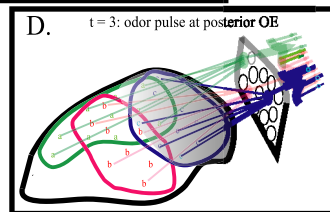
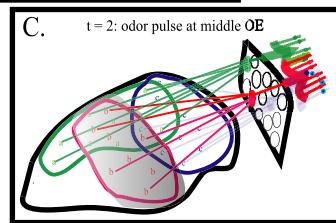
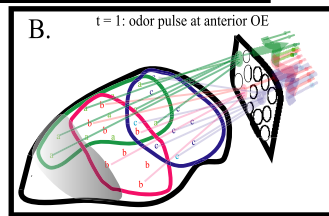
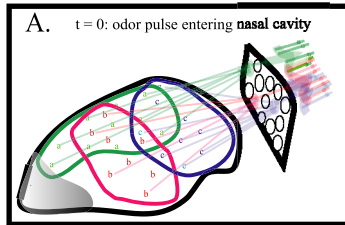
17. Convergence of input from multiple identical sensors is used to improve signal to noise ratio.

18. Analytical algorithms are based on biological neuronal circuits

19. Recognition and identification emerge from repeated (and continuous) training with feedback ('reward' contingency).

20. Recognition templates are stored in a library in random access memory.

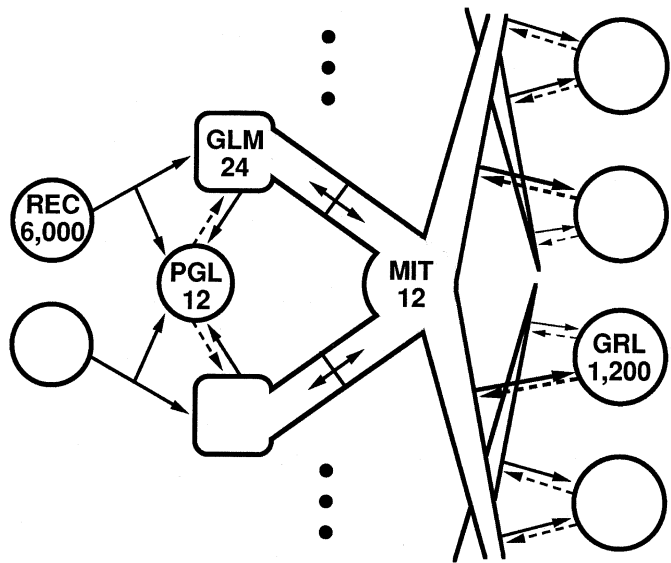
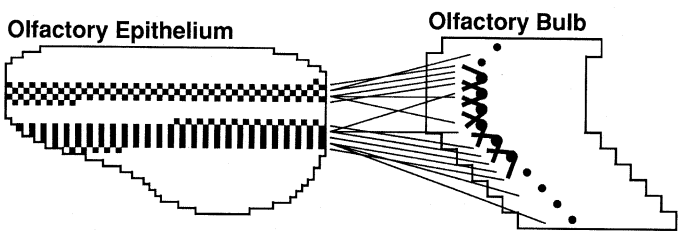
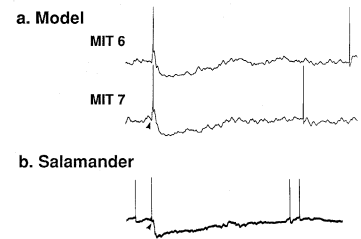
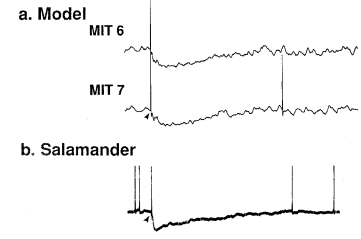
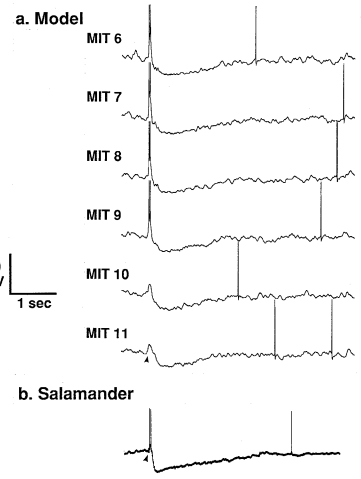
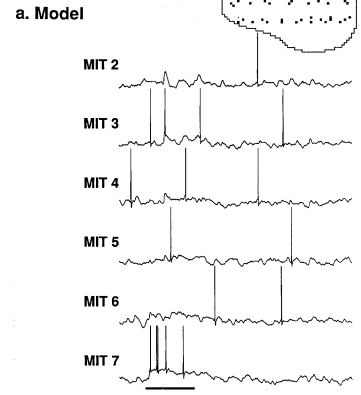
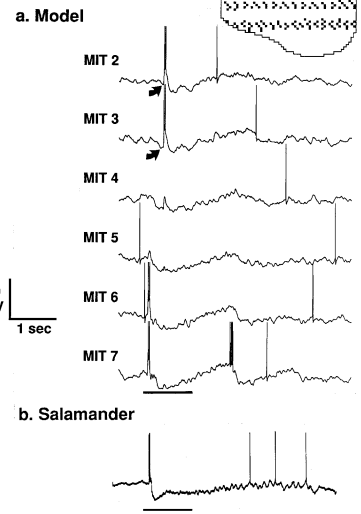
21. Output is by spoken word.

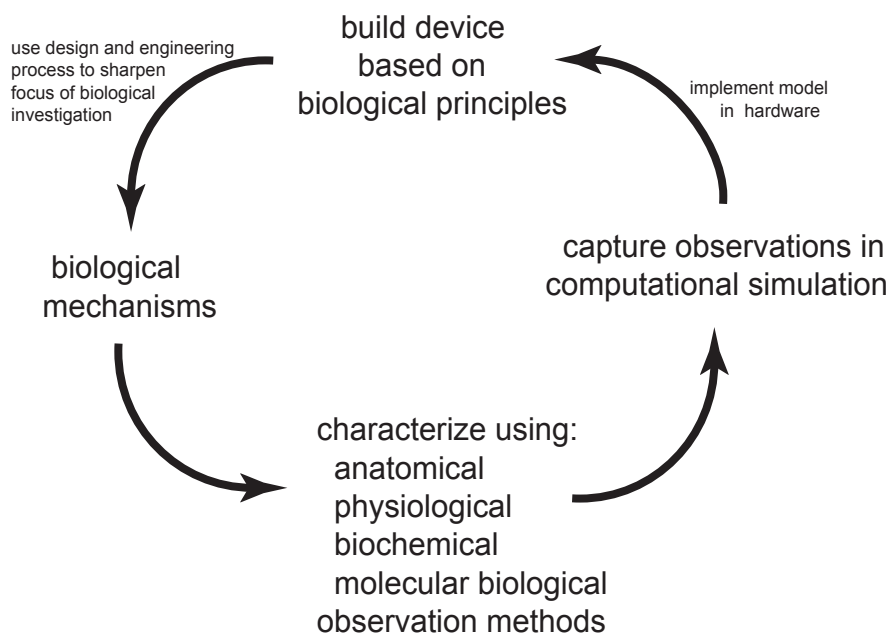


Spatial and Temporal,
Combinatorial Odorant
Coding

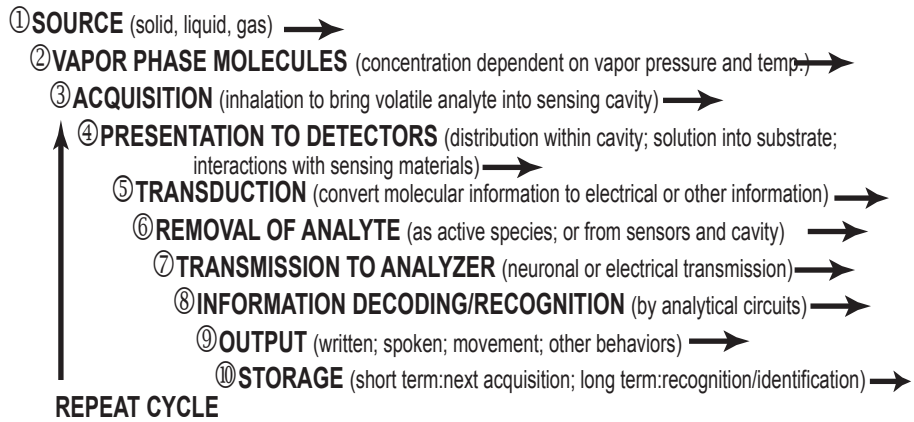
a, b, c = receptors for recognition sites



A.**B.****A. Low Intensity Orthodromic****C. Antidromic****B. High Intensity Orthodromic****A. Low Intensity Odor****B. High Intensity Odor**



A.



B.

